Gene Expression Profiles of Nondiabetic and Diabetic Obese Mice Suggest a Role of Hepatic Lipogenic Capacity in Diabetes Susceptibility

Hong Lan,[1] Mary E. Rabaglia,[1] Jonathan P. Stoehr,[1] Samuel T. Nadler,[1] Kathryn L. Schueler,[1] Fei Zou,[2] Brian S. Yandell,[3] and Alan D. Attie[1]

Obesity is a strong risk factor for the development of type 2 diabetes. We have previously reported that in adipose tissue of obese (*ob/ob*) mice, the expression of adipogenic genes is decreased. When made genetically obese, the BTBR mouse strain is diabetes susceptible and the C57BL/6J (B6) strain is diabetes resistant. We used DNA microarrays and RT-PCR to compare the gene expression in BTBR-*ob/ob* versus B6-*ob/ob* mice in adipose tissue, liver, skeletal muscle, and pancreatic islets. Our results show: *1*) there is an increased expression of genes involved in inflammation in adipose tissue of diabetic mice; *2*) lipogenic gene expression was lower in adipose tissue of diabetes-susceptible mice, and it continued to decrease with the development of diabetes, compared with diabetes-resistant obese mice; *3*) hepatic expression of lipogenic enzymes was increased and the hepatic triglyceride content was greatly elevated in diabetes-resistant obese mice; *4*) hepatic expression of gluconeogenic genes was suppressed at the prediabetic stage but not at the onset of diabetes; and *5*) genes normally not expressed in skeletal muscle and pancreatic islets were expressed in these tissues in the diabetic mice. We propose that increased hepatic lipogenic capacity protects the B6-*ob/ob* mice from the development of type 2 diabetes. *Diabetes* 52:688–700, 2003

Type 2 diabetes is characterized by hyperglycemia resulting from a failure of the pancreatic β-cells to compensate for insulin resistance. Obesity, which leads to insulin resistance, is a strong risk factor for the development of type 2 diabetes. However, only ~20% of obese people develop diabetes; most obese people can maintain euglycemia throughout their life span, despite insulin resistance. Genetic factors play a role in determining whether an obese individual develops type 2 diabetes. It is therefore important to understand the differences underlying the two types of obesity: that which resists the onset of diabetes and that which is linked to diabetes.

We studied the link between obesity and diabetes using two mouse models of obesity. The C57BL/6J (B6)-*ob/ob* mouse strain, despite extreme obesity and insulin resistance, develops only mild, transient hyperglycemia under a regular chow diet (1,2). Lean BTBR mice are insulin resistant (3). When the *ob* mutation is introgressed onto the BTBR background through repeated backcrossing and selection of the *ob* allele (2), the BTBR-*ob/ob* mice develop severe diabetes. The fasting plasma glucose reaches 400 mg/dl at 10 weeks of age, whereas for age-matched B6-*ob/ob* mice, glucose remains <250 mg/dl (2).

The expression of adipogenic genes, including the transcription factor adipocyte determination factor 1/sterol regulatory element binding protein (ADD1/SREBP), is decreased in adipose tissue of *ob/ob* mice (4,5). These studies suggest that adipocytes in obese adipose tissue have a reduced lipogenic capacity. This has been confirmed in adipose tissue of obese human subjects (6–9). On the other hand, in mouse models of extreme leanness (lipodystrophy) and extreme obesity (*ob/ob*), hepatic expression of SREBP1 and lipogenic target genes involved in fatty acid biosynthesis are increased, leading to significantly higher rates of hepatic fatty acid synthesis in vivo (10). In human obesity, decreased lipogenic gene expression in adipose tissue is coupled with increased hepatic lipogenesis (8). These findings suggest that reduced lipogenic adipocytes, or perhaps adipocyte dysfunction, is associated with increased hepatic lipogenesis. We hypothesized that there is a shift in the "lipogenic burden" from adipose tissue to other organs, such as the liver, in animals with less lipogenic adipose tissue (11). It is unclear whether this shift is adaptive or pathological with regard to diabetes. In this study, we show that resistance to diabetes correlates with a high level of hepatic lipogenic gene expression and hepatic steatosis in B6-*ob/ob* mice, and that a failure to increase hepatic lipogenesis may contribute to diabetes in BTBR-*ob/ob* mice.

RESEARCH DESIGN AND METHODS

Animals. B6, BTBR, B6-*ob/+*, and B6-*ob/ob* mice were purchased from The Jackson Laboratory (Bar Harbor, ME). The BTBR-*ob/ob* congenic line was created in our laboratory by introgressing the *ob* mutation from the B6 mice onto the BTBR background (2,3). All mice were maintained at the University
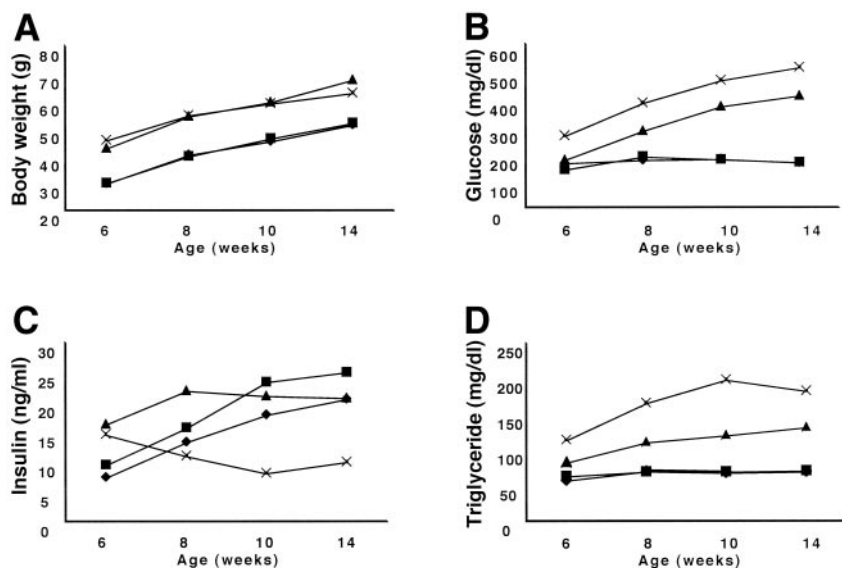
FIG. 1. Phenotype of *ob/ob* mice by sex and genetic background, from 6 to 14 weeks of age. Body weight (*A*), fasting glucose (*B*), fasting insulin (*C*), and fasting (*D*) TG level are reported for each mouse. ◆, B6-*ob/ob* female mice (*n* = 62); ■, B6-*ob/ob* male mice (*n* = 62); ▲, BTBR-*ob/ob* female mice (*n* = 87); ✕, BTBR-*ob/ob* male mice (*n* = 56). Average values were plotted. Missing data were possible for some points; for example, for animals that were killed at 6 weeks of age, there were no data for time points >6 weeks.

of Wisconsin-Madison animal care facility on a 12-h light/dark cycle. The mice were provided Purina Formulab Chow 5008 (6.5% fat) and acidified water ad libitum. Mice were fasted for 4 h before blood withdrawal to measure plasma glucose, insulin, and triglyceride (TG) levels. The University of Wisconsin-Madison institutional animal care and use committee approved all protocols.

RNA preparation. Mice were killed by CO_2 asphyxiation after a 4-h fast. Abdominal fat pads, liver, and soleus muscle were quickly transferred into liquid N_2 and stored at $-80°C$. Total RNA was extracted from the three tissues with RNAzol reagent (Tel-Test). Intact islets were isolated from pancreas using a collagenase digestion procedure and were handpicked under a stereomicroscope. Isolated islets from each individual were preserved in TriReagent (Molecular Research Center, Cincinnati, OH) at $-80°C$ until RNA preparation. Crude RNA samples were purified with RNeasy mini columns (Qiagen) before being subjected to microarray and RT-PCR studies.

Microarrays. Four B6-*ob/ob* and four BTBR-*ob/ob* male mice at 14 weeks of age were used in the microarray study. RNA samples from two animals were pooled for each tissue, and each pooled RNA sample was applied to an Affymetrix MGU74A array. Because of the scarcity of islets in the BTBR-*ob/ob* mice, four additional mice were pooled to obtain islet RNA from these animals. A total of 16 MGU74Av2 arrays (2 strains × 4 tissues × 2 replicates = 16 arrays) were used to monitor the expression level of ∼12,000 genes or expressed sequence tags. The data were processed with Affymetrix Microarray Suite 4.0. Quantitative expression levels of all the transcripts were estimated using the DNA-Chip analyzer (dChip) algorithm (12). dChip models probe level data to account for artifacts such as probe-specific biases. Corrected and normalized model-based estimates of gene expression were obtained. Genes that are differentially expressed between the B6-*ob/ob* mice and the BTBR-*ob/ob* mice were determined using a statistical algorithm accounting for measurement errors and fluctuations in absolute gene expression levels (developed by Y. Lin and B.S.Y., University of Wisconsin-Madison) (13). Briefly, the raw-expression data are rank ordered by values. The ranks are converted into normal scores by stratifying into quintiles. The expression levels for each gene across experimental samples are then calculated using the normal scores. Differential expression across conditions of interest is computed by contrasting the normal scores between conditions. Robust estimates of center and spread varying across the average intensity are computed using smoothed medians and smoothed median absolute deviations, respectively. The contrasts of differential expression are standardized using the calculated center and spread. Fold changes are calculated based on the normal scores instead of raw expression data.

These standardized values should have an approximately standard normal distribution for genes that are not differentially expressed. *P* values are derived using a Bonferroni-style genome-wide correction. The software can be found online at http://www.stat.wisc.edu/~yandell/statgen. By using normal scores and the center and spread algorithm, the method robustly adapts to changing variability across average expression levels. Upon identification of differentially expressed genes, the patterns of gene expression were tentatively assembled based on our current knowledge of gene functions.

Real-time quantitative PCR. RNA samples from individual mouse tissues were used for RT-PCR. First-strand cDNA was synthesized from 1 μg of total RNA using Super Script II RT (Gibco BRL) primed with a mixture of oligo-dT and random hexamers. Reactions lacking the reverse transcriptase served as

a control for amplification of genomic DNA. Unless otherwise specified, the reaction was carried out in a 25-μl volume in 1 × SYBR Green PCR core reagents (Applied Biosystems) containing cDNA template from 10 ng of total RNA and 6 pmol of primers. Quantitative PCR was performed on an ABI GeneAmp 5700 sequence detection system. For each gene, the cDNA samples were gridded onto a 96-well plate. For each sample, at least duplicate amplifications were performed and average measurements were taken for data analysis.

We determined the cycle at which the abundance of the accumulated PCR product crosses a specific threshold, the threshold cycle (C_T) for each reaction. The difference in average C_T values between β-actin and a specific gene was calculated for each individual and is termed ΔC_T, which is comparable to the log-transformed, normalized mRNA abundance. In some instances, ΔC_T values were further converted to relative expression levels normalized against the mean expression in B6-*ob/ob* mice. All values are presented as the means ± SD. Comparisons were evaluated by Student's *t* test (two tailed).

Liver TG content. Tissue TG content was measured with an assay based on the detection of glycerol (14). Briefly, frozen liver tissue (10–30 mg) was minced in chloroform and methanol (2:1 ratio). Minced samples were incubated at $-20°C$ overnight to release lipid before centrifugation at 1,200 rpm for 10 min at 4°C to remove tissue debris. The supernatants were washed with H_2O to remove water-soluble components. Lipids in the organic phase were transferred into a new tube, dried, and redissolved with Thesit (Fluka). TG was assayed using the GPO Trinder reagent (Sigma).

RESULTS

The primary objective of this study was to identify the differences in gene expression between obese nondiabetic and obese diabetic mice. Figure 1 shows the plasma phenotypes of B6-*ob/ob* and BTBR-*ob/ob* mice. As we have previously reported (2), the BTBR-*ob/ob* mice are diabetic, whereas B6-*ob/ob* mice are not. B6-*ob/ob* mice showed slightly increased fasting glucose at 8 weeks of age, but they returned to a plateau at 10 weeks (Fig. 1*B*). The euglycemia was maintained with progressive hyperinsulinemia (Fig. 1*C*). These mice also maintained normal plasma TG levels (Fig. 1*D*). In contrast, BTBR-*ob/ob* mice developed severe diabetes. However, female BTBR-*ob/ob* mice do not show hyperglycemia until after 6 weeks of age, probably because they maintain insulin compensation until 8 weeks. We therefore used 6-week-old female BTBR-*ob/ob* mice to study prediabetic changes, together with age- and sex-matched B6-*ob/ob* mice as controls. The mice also have hypertriglyceridemia that progresses between 6 and 14 weeks of age (Fig. 1*D*).
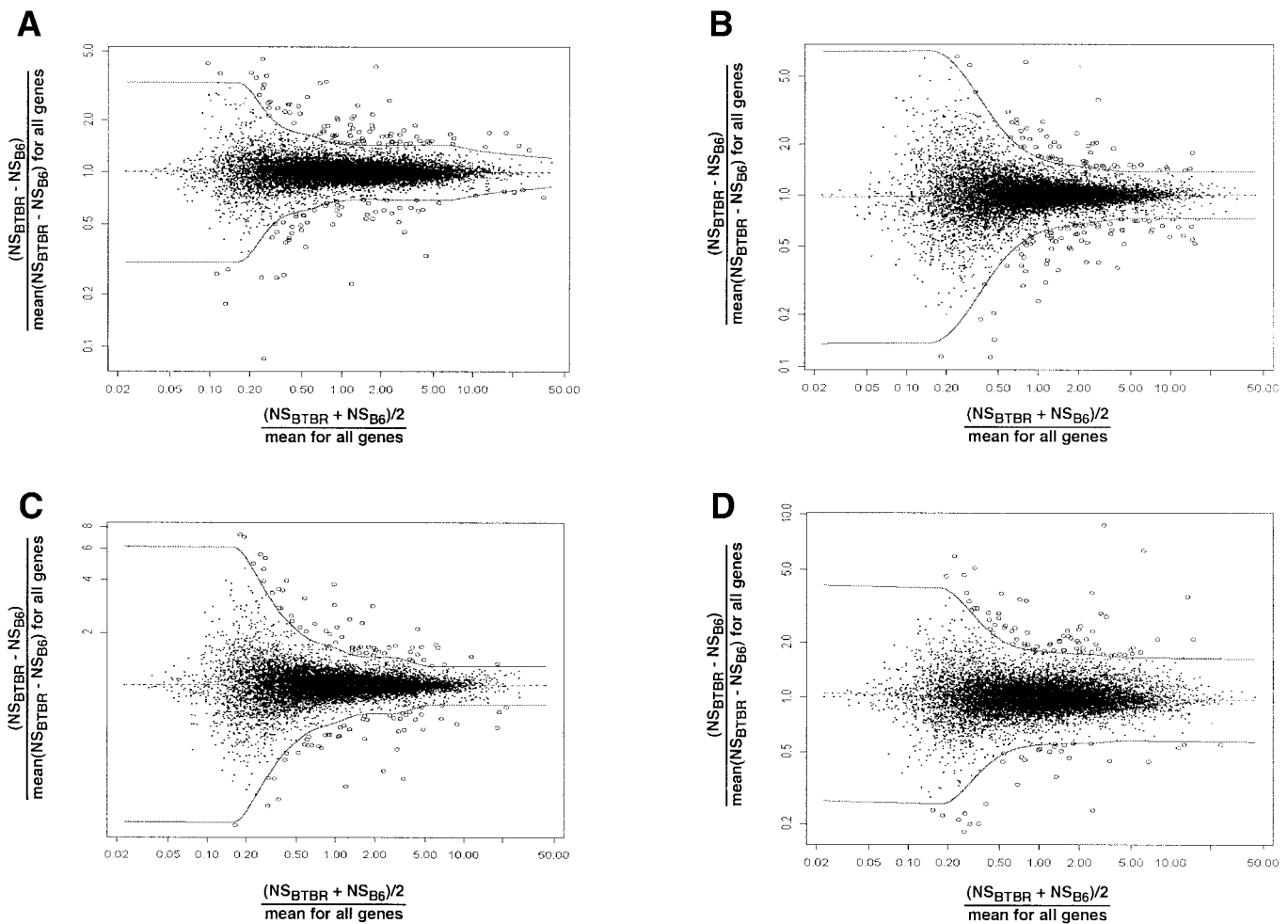
FIG. 2. Genes that are significantly differentially expressed in adipose tissue (*A*), liver (*B*), muscle (*C*), and islet (*D*) between B6-*ob/ob* and BRBT-*ob/ob* mice were identified using a statistical algorithm accounting for measurement errors and fluctuations in absolute gene expression levels. The *x*-axis reflects the normalized expression level, and the *y*-axis reflects differential expression, as described in the RESEARCH DESIGN AND METHODS section. The solid line in each graph indicates the significant threshold ($P < 0.05$). ○, Genes exceeding the 5% criteria.

Although female BTBR-*ob/ob* mice are not different from B6-*ob/ob* mice in glucose level at 6 weeks of age ($P = 0.4$, $n = 45$ vs. 68), they already show a significantly higher plasma TG level (97.6 ± 34.7 mg/dl, $n = 41$) than B6-*ob/ob* mice (72.3 ± 23.7, $n = 68$; $P < 0.0001$). Thus, it appears that hypertriglyceridemia precedes the onset of hyperglycemia (Fig. 1).

Microarrays were used to study gene expression in adipose tissue, liver, skeletal muscle, and pancreatic islets. Duplicate samples from 14-week-old male mice were used because they show the greatest phenotypic difference between B6-*ob/ob* and BTBR-*ob/ob* mice (Fig. 1). Of the 12,421 transcripts represented on the Affymetrix Mouse Genome U74A V2 arrays, 5,629 (45%) were expressed in adipose tissue (called "present" by Affymetrix software), and 4,218 (34%), 4,472 (36%), and 4,697 (38%) were expressed in liver, muscle, and islets, respectively. There was no strain difference regarding how many genes were expressed in each of the four tissues.

To identify transcripts as differentially expressed between experimental conditions, a procedure that simply uses an arbitrary fold change ratio cutoff is no longer considered effective because it ignores the fact that the variation of such ratios is not consistent across absolute

expression levels (15). In this study, we used a new algorithm that uses a significance threshold that varies as a function of absolute expression level rather than an arbitrary fold change value. Figure 2 shows the dot graphs of genes identified as differentially expressed between B6-*ob/ob* and BTBR-*ob/ob* in each of the four tissues. Note that in Fig. 2, the lines defining significance thresholds address the variations in microarray data better than straight fold-change lines would. For low-abundance genes, a greater change is required to cross the significance threshold.

We identified 149 transcripts in adipose tissue, 142 in liver, 111 in skeletal muscle, and 105 in pancreatic islets, respectively, as differentially expressed between B6-*ob/ob* and BTBR-*ob/ob*. The transcripts with functional annotations are listed in Tables 1–4. The complete microarray dataset is available in the online supplement at http://diabetes.diabetesjournals.org.

In adipose tissue, the expression levels of adipogenic genes, including lipogenic genes, were similar between 14-week-old male B6-*ob/ob* and BTBR-*ob/ob* mice, except for a few genes such as adipsin/complement D (16), whose mRNA abundance was reduced in BTBR-*ob/ob* (Table 1).

The data suggest that hyperglycemia or hypertriglyceri-

TABLE 1
Genes differentially expressed in adipose tissue in diabetic BTBR-*ob/ob* mice

Accession	Description	Fold	*P*
Downregulated in BTBR-*ob/ob*			
Adipocyte differentiation			
X04673	Adipsin (Complement D)	−2.2	<0.0001
AF053943	Adipocyte-enhancer binding protein	−2.5	<0.0001
Signal transduction			
X76290	Sonic hedgehog homolog	−2.4	<0.0001
M60596	GABA-A receptor delta-subunit gene	−2.0	<0.0001
AF047716	Kinase anchor protein 7 (Akap 18)	−2.0	<0.0001
AB016080	Kinase interacting protein 2 (Kip2)	−1.9	<0.0001
AW046879	ACP33 (acidic cluster protein 33)	−1.8	<0.0029
M31312	Fc receptor, IgG, low affinity IIb	−1.7	<0.0001
AF036585	Semaphorin 6B	−1.8	<0.0001
U67188	Regulator of G-protein signaling 5	−1.5	0.0363
U60473	CD59a antigen	−2.0	<0.0001
AA960657	Interferon activated gene 203	−1.5	0.0187
X99347	Lipopolysaccharide binding protein	−1.6	<0.0001
Metabolism			
Z22216	Apolipoprotein CII	−1.5	0.0354
AB003305	Proteasome subunit, beta type 5	−1.6	<0.0001
L42115	Adipocyte amino acid transporter	−4.4	<0.0001
Others			
X05862	H2B histone gene	−3.0	<0.0001
D88792	Cysteine-rich protein 2	−1.7	<0.0001
AV013428	Crystallin, alpha 2	−1.7	<0.0001
U72032	Eosinophil-associated ribonuclease 1	−1.6	0.0107
AB031291	Neuronal protein NP25	−1.6	0.0002
L23971	Fragile X mental retardation syndrome 1	−1.7	<0.0001
AW124972	DNA segment, ERATO Doi 21, expressed	−1.6	0.0014
AF017994	Peg1/MEST protein	−1.7	<0.0001
C78850	Envelope protein (env) gene	−1.6	<0.0001
Upregulated in BTBR-*ob/ob*			
Inflammatory			
M75721	Serine protease inhibitor 1-1	1.9	<0.0001
M25529	Serine protease inhibitor 1-2	4.1	<0.0001
M75720	Serine protease inhibitor 1-3	1.7	<0.0001
M75718	Serine protease inhibitor 1-4	2.1	<0.0001
M75717	Serine protease inhibitor 1-5	2.0	<0.0001
X00945	Serine protease inhibitor 1-6	3.2	<0.0001
X70296	Serine proteinase inhibitor, clade E	1.5	0.0267
AF030636	Cytokine subfamily B 13	3.3	<0.0001
M31418	Interferon activated gene 202A	2.5	<0.0001
AJ007971	Interferon-inducible GTPase	2.6	<0.0001
AF035684	Small inducible cytokine A21a (leucine)	1.8	<0.0001
X70058	Small inducible cytokine A7	1.6	0.0002
AB001607	Prostaglandin 12 synthase	1.7	<0.0001
D10204	Prostaglandin E receptor 3	1.5	0.0293
Metabolism			
AJ001418	Pyruvate dehydrogenase kinase 4	1.9	<0.0001
AF009605	Phosphoenolpyruvate carboxykinase 1	1.5	0.0018
M74570	Alcohol dehydrogenase family 1	1.5	0.0107
AA144642	Fructose 1,6-bisphosphate aldolase	1.6	0.0001
X61172	Mannosidase 2, alpha 1	1.6	<0.0001
Y12887	Carboxylesterase 1	2.5	<0.0001
AW226939	Esterase 1	1.7	<0.0001
L16992	Ketoacid dehydrogenase E1	1.6	<0.0001
L07645	Histidine ammonia lyase	2.7	<0.0001
U51805	Arginase 1	2.0	<0.0001
Y08027	ART3	1.5	0.0042
M55544	Guanylate nucleotide binding protein 1	1.9	<0.0001
Signal transduction			
AF024621	γ-aminobutyric acid receptor	1.8	<0.0001
AF071180	Formyl peptide receptor, related 2	2.2	<0.0001
AJ010045	Guanine nucleotide regulatory protein	1.6	<0.0001
X60367	Retinol binding protein 1, cellular	1.5	0.0265

TABLE 1
Continued

Accession	Description	Fold	P
Others			
M27134	Histocompatibility 2, K region locus 2	2.4	<0.0001
AJ243851	LIM homeobox protein 9	1.7	0.0019
X83601	Pentaxin related gene	1.6	0.0001
X83569	Neuronatin	1.7	<0.0001
AF038939	Paternally expressed gene 3	1.6	<0.0001
M16238	Fibrinogen-like protein 2	1.5	0.0021
AA647799	Osteoglycin	1.5	0.0228
L12367	Adenylyl cyclase-associated CAP protein	1.5	0.0442
X65128	Growth arrest specific 1	1.5	0.0026
AB020886	Src Suppressed C Kinase Substrate	1.5	0.0013
M91380	Follistatin-like	1.5	0.0040
M96827	Haptoglobin	1.7	<0.0001

demia in 14-week-old BTBR-*ob/ob* mice has no discernible effect on adipogenesis or lipogenesis in adipose tissue. On the other hand, mRNAs for a number of genes generally expressed in macrophages or inflammatory cells were increased in diabetic BTBR-*ob/ob* mice, including a group of α1-serine protease inhibitors, as well as some cytokines and interferon-induced genes (Table 1). The data reveals a previously unappreciated abnormality in diabetic adipose tissue.

In the liver, genes involved in the lipogenic pathway were markedly downregulated in the diabetic BTBR-*ob/ob* mice (Table 2). The genes include fatty acid synthase (*FAS*), stearoyl coenzyme A desaturase 1 (*SCD1*), glycerol-3-phosphate acyltransferase (*GPAT*), malic enzyme, the LDL receptor, sterol-C5-desaturase, and *SPOT14*, a known *SREBP1* target gene. The data strongly suggest that lipogenesis is reduced in the liver of obese diabetic mice compared with obese nondiabetic mice.

In skeletal muscle, several adipocyte marker genes showed higher expression in BTBR-*ob/ob* mice. These include genes known to be expressed exclusively in adipose tissue, such as *aP2*, adipsin, adipocyte complement–related protein of 30 kDa (*ACRP30*), fasting-induced adipose factor (*FIAF*; fibrinogen/angiopoietin-related protein), as well as lipogenic genes such as *SCD1* (Table 3). It is most likely that these mRNAs represent an increased level of adipose tissue in the muscle of the diabetic mice.

Finally, genes that are not normally expressed or are expressed at lower levels in pancreatic islets are more highly expressed in diabetic BTBR-*ob/ob* islets, including fructose-1, 6-bisphosphatase 1 (*FBPase1*), *FBPase2*, and cholecystokinin (Table 4). On the other hand, *GLUT2* mRNA was found to be lower in BTBR-*ob/ob* islets, although the difference did not reach our strict threshold of significance. Interestingly, the expression of the fatty liver dystrophy gene *lipin* (17) increased by 2.5-fold in diabetic BTBR-*ob/ob* islets.

Low-abundance signals on microarrays are subject to high variability (15). High-abundance genes are subject to signal saturation because of the detection limit of the laser scanners. We noticed that very-low-abundance transcription factors such as *SREBP1* or peroxisome proliferator–activated receptor-γ (*PPAR-γ*) did not show significant differential expression on microarrays. In addition, important lipogenic genes, such as acetyl CoA carboxylase (*ACC*) or malonyl CoA decarboxylase (*MCD*), were not

represented on MGU74 arrays. For these reasons, we used quantitative RT-PCR to confirm our observations from the microarray study and also to expand our investigation on the altered gene expression profiles. Apart from its wide dynamic range of detection, RT-PCR can efficiently measure mRNA abundance of multiple individuals and thereby increase the power of statistical tests to compare two experimental groups.

Because our microarray study was carried out using 14-week-old male mice, we cannot determine whether the changes are causes or consequences of diabetes. Some changes may have been blunted under chronic hyperglycemia so that they are not detectable with microarrays. To identify gene expression changes that precede the onset of diabetes, we chose to study prediabetic 6-week-old female mice (Fig. 1*B*). We assume the differences seen in the prediabetic mice would likely be causative of diabetes, whereas those seen after the onset of diabetes would more likely be adaptive. Six BTBR-*ob/ob* mice (fasting glucose 200 mg/dl) were compared with eight B6-*ob/ob* mice (fasting glucose 220 mg/dl). Because the microarray studies indicated reduced lipogenic gene expression in the liver, we studied genes involved in lipogenesis. To expand our previous study in adipose tissue comparing lean and obese mice (5), we also included lean mice in this study. Below, we describe the results of these analyses.

Reduction of lipogenic gene expression in adipose tissue of obese and diabetic mice. The expression of *aP2*, *adipsin*, *ACRP30*, and *FIAF* decreased dramatically in obese mice (Fig. 3*A*). The mRNA abundance of adipogenic transcriptional factors such as *PPAR-γ* and *SREBP1* also dropped. Adipsin mRNA was also significantly lower in BTBR-*ob/ob* adipose tissue compared with B6-*ob/ob*.

We found decreased lipogenic gene expression in prediabetic adipose tissue. The expression of *SREBP1* and its target genes, including *ACC*, *FAS*, and *SCD1*, were significantly lower in adipose tissue of BTBR-*ob/ob* mice at 6 weeks of age (Fig. 3*B*). *PPARγ* and *GPAT* were regulated in the opposite direction. No strain difference was observed at 14 weeks of age. The expression of two representative lipogenic genes, *SCD1* and *FAS*, decreased dramatically from 6 to 14 weeks in both strains (Fig. 3*C*). Thus, the absence of a difference at 14 weeks was caused by a greater decrease in B6-*ob/ob* mice. Our data suggest that adipose function, reflected by the expression of lipogenic genes, deteriorates with prolonged obesity.

TABLE 2
Genes differentially expressed in liver in diabetic BTBR-*ob/ob* mice

Accession	Description	Fold	*P*
Downregulated in BTBR-*ob/ob*			
Lipogenesis			
X13135	Fatty acid synthase	−1.4	0.0032
M21285	Stearoyl-coenzyme A desaturase 1	−1.5	<0.0001
U11680	Glycerol-3-phosphate acyltransferase	−1.6	<0.0001
J02652	Malic enzyme	−1.5	0.0269
Z19521	LDL receptor	−1.4	0.0258
X95279	SPOT14 homolog	−1.6	<0.0001
AB016248	Sterol-C5-desaturase	−2.5	<0.0001
U28960	Phospholipid transfer protein	−2.1	<0.0001
Metabolism			
M21855	Cytochrome P450, 2b9	−2.0	<0.0001
X63023	Cytochrome P450 3a13	−1.9	<0.0001
M21856	Cytochrome P450, 2b10	−1.9	<0.0001
AW047343	D site albumin promoter binding protein	−2.6	<0.0001
U89906	α-methylacyl-CoA racemase	−1.9	<0.0001
AI047508	Arylacetamide deacetylase	−1.6	<0.0001
Y12887	Carboxylesterase 1	−1.6	<0.0001
AJ132098	Vanin 1/panletheinase	−1.5	0.0016
AI326397	Glutathione S-transferase, mu 6	−1.7	<0.0001
M88694	Thioether S-methyltransferase	−1.7	<0.0001
AB027012	Galactokinase	−1.6	0.0029
M63245	Amino levulinate synthase (ALAS-H)	−1.4	0.0022
Immune response			
M35525	Hemolytic complement (C5)	−4.2	<0.0001
D89290	CD151 antigen	−2.8	<0.0001
AF001277	Chemokine (C-C) receptor 8	−1.9	<0.0001
AI854154	ACP33 (acidic cluster protein 33)	−1.7	0.0008
D64162	Rae1	−1.7	<0.0001
M27008	Orosomucoid 1	−1.5	<0.0001
M13521	Serum amyloid A 1	−1.9	<0.0001
U60438	Serum amyloid A 2	−1.4	0.0091
Extracellular matrix			
U03419	Procollagen, type 1, alpha 1	−2.4	<0.0001
X52046	Procollagen, type III, alpha 1	−1.9	0.0101
X15986	Lectin, galactose binding, soluble 1	−2.7	<0.0001
Signal transduction			
U94828	Regulator of G-protein signaling 16	−1.5	0.0002
AF041376	DNA fragmentation factor	−2.5	<0.0001
AV115237	Translation initiation factor 4E	−2.8	<0.0001
X83577	Glypican 4	−1.9	0.0009
Others			
AV355798	Major urinary protein 1	−1.8	<0.0001
AI255271	Major urinary protein 1	−1.5	<0.0001
M16357	Major urinary protein 3	−1.8	<0.0001
M16358	Major urinary protein 4	−1.4	0.0134
M16360	Major urinary protein 5	−1.4	0.0466
AF018952	Aquaporin 8	−1.5	0.0024
AI120514	Sulfate anion transporter (sat-1)	−1.8	0.0001
X05862	Mouse H2B histone gene	−2.5	<0.0001
AI848902	Ribosomal protein L14 (60S subunit)	−2.0	0.0020
M64292	B-cell translocation gene 2	−1.8	<0.0001
AB003305	Proteasome subunit, beta type 5	−1.7	<0.0001
AI530403	DNA segment ERATO Doi 25, expressed	−1.5	0.0009
Upregulated in BTBR-*ob/ob*			
Immune response/signal transduction			
X03505	Serum amyloid A3	3.6	<0.0001
D00725	Serine protease inhibitor 2	2.0	<0.0001
X05475	Complement component 9	1.5	<0.0001
AF031127	Inositol trisphosphate receptor 2 (Itpr2)	1.7	0.0228
AW049716	Epidermal growth factor receptor	1.6	0.0006
AI835443	c-myc, exon 2	1.5	0.0141
AB012808	Organic cation transporter	1.9	<0.0001

Continued on following page

TABLE 2
Continued

Accession	Description	Fold	P
Structure			
Y07711	Zyxin	2.1	<0.0001
AF020185	Dynein, cytoplasmic, light chain 1	1.6	0.0004
L31397	Dynamin	1.4	0.0387
Others			
M58567	Hydroxysteroid dehydrogenase-1	2.6	<0.0001
AF059177	Avian erythroblastosis oncogene B 4	2.7	<0.0001
AV368725	Fragile X mental retardation gene	2.2	<0.0001
M17327	Provirus envelope protein	1.9	<0.0001
AV084197	Activating transcription factor 3	1.9	0.0002
D13803	RecA-like protein murine Rad51	1.9	<0.0001
AJ009840	Cathepsin E/lysosomal protease	1.6	0.0032
X91864	Glulathione peroxidase 2	1.5	0.0002
AI840339	Ribonuclease, RNase A family 4	1.5	0.0004

Hepatic steatosis in diabetes-resistant B6-*ob/ob* mice. We compared gene expression in the livers of the two obese mouse strains. Decreased lipogenic gene expression was seen in BTBR-*ob/ob* liver at both the prediabetic and the diabetic stages (Figs. 4*A* and *B*). The reduction at 14 weeks was even greater (Fig. 4*B*). Unlike that in adipose tissue, the expression of *SCD1* and *FAS* in the liver of B6-*ob/ob* mice did not decrease with age (Fig. 4*C*). The data suggest that the liver of B6-*ob/ob* mice maintains a high level of hepatic lipogenesis. In contrast, hepatic lipogenic gene expression remained low from the prediabetic to the diabetic stages in BTBR-*ob/ob* mice compared with insulin-resistant but nondiabetic B6-*ob/ob* mice.

We measured liver TG content in the two obese mouse strains at 6 and 14 weeks of age (Fig. 4*D*). Consistent with the gene expression data, the liver TG content of B6-*ob/ob* mice was increased 3.5-fold ($P < 0.001$) at 6 weeks and 5.3-fold ($P < 0.001$) at 14 weeks, respectively, compared with the age-matched BTBR-*ob/ob* mice. Hepatic steatosis increased dramatically from 6 to 14 weeks in B6-*ob/ob* mice, although the mice maintained euglycemia. In contrast, the liver TG content in BTBR-*ob/ob* mice remained low during the time they developed severe hyperglycemia. **Other changes of gene expression in diabetic BTBR-*ob/ob* mice.** Reduced expression of fatty acid oxidation genes was also observed in multiple organs of obese diabetic mice. Acyl CoA oxidase (ACO) is an enzyme involved in the first step of the peroxisomal fatty acid oxidation pathway. In adipose tissue and soleus muscle, ACO expression decreased by 8.6- and 11.5-fold, respectively, in obese mice compared with lean mice ($P < 0.01$) (Fig. 5*A*). There was a further reduction in the soleus muscle of BTBR-*ob/ob* relative to B6-*ob/ob* ($P < 0.05$) (Fig. 5*A*, right panel). In liver, a strain difference was observed with BTBR-*ob/ob* mice showing an 80% reduction at 6 weeks and a 70% reduction at 14 weeks. Thus, the reduction precedes the onset of diabetes in BTBR-*ob/ob* mice. In each strain, the expression of ACO also decreased when animals aged (Fig. 5*B*). The data suggest that the obese mice have reduced fatty acid oxidation, and that there was further reduction in diabetic mice. Despite the change in ACO expression, we did not observe any change in the expression of the transcriptional factor PPAR-α. It is likely that PPAR-α activity, rather than its mRNA level, mediate changes in lipid oxidation during the development of diabetes. The expression of gluconeogenic genes in BTBR-*ob/ob* liver was suppressed at 6 weeks but not at 14 weeks (Fig. 6). At 6 weeks, three key genes in the gluconeogenic pathway were expressed at a reduced level in BTBR-*ob/ob* mice, although only *FBPase1* reached a significant level (Fig. 6*A*). An opposite trend was observed at 14 weeks; phosphoenopyruvate carboxykinase (*PEPCK*) was expressed at a significantly higher level in BTBR-*ob/ob* (Fig. 6*B*). This suggests an increase in hepatic gluconeogenesis at the onset of diabetes in BTBR-*ob/ob* mice.

DISCUSSION

In this study, we compared gene expression between two mouse models of obesity—one that develops severe diabetes (BTBR-*ob/ob*) and one that is diabetes resistant (B6-*ob/ob*). Our results suggested a pathophysiological cascade of type 2 diabetes in the mouse models: *1*) there is an increased expression of inflammatory mediators in adipose tissue; *2*) the increased inflammation mediators could impair adipose lipogenesis through paracrine effects and/or prevent an induction of the same processes in liver through endocrine effects; and *3*) the failure to increase hepatic lipogenesis in the liver is associated with in an increase in hepatic glucose production.

Microarray technology is a useful tool to detect novel aspects of disease-associated gene expression patterns. Soukas et al. (4) reported increased expression of inflammatory genes and acute-phase proteins, such as serum amyloid A3 and A4, LPS binding protein, and SV40-induced 24p3, in adipose tissue as well as in isolated adipocytes of leptin-deficient mice. The data suggest a possible link between immune system function and obesity. In the present study, multiple genes encoding α1-serine protease inhibitors, including types 1-1 through 1-6, showed coordinately elevated expression in adipose tissue of the diabetic BTBR-*ob/ob* mice (Table 1*A*). The inhibitors are antitrypsin peptides (18). Deficiency in these genes leads to early onset emphysema (19). These genes are expressed predominantly in macrophages and in the liver, and high protein concentrations are present in plasma. Additional inflammatory response genes are also found to be more

TABLE 3
Genes differentially expressed in skeletal muscle in diabetic BTBR-*ob/ob* mice

Accession	Description	Fold	*P*
Downregulated in BTBR-*ob/ob*			
Structure			
AV359510	Actinin alpha 3	−2.3	<0.0001
AF093775	Actinin alpha 3	−1.8	<0.0001
J04992	Troponin 1, skeletal, fast 2	−1.5	<0.0001
AJ223361	Myosin heavy chain 2B	−3.4	<0.0001
AJ002522	Myosin heavy chain 2X	−1.7	<0.0001
U04541	Tropomyosin 5	−1.7	<0.0001
Others			
X59382	Parvalbumin	−3.8	<0.0001
X05862	H2B histone gene	−3.1	<0.0001
AI850569	Pyrroline 5-carboxylate reductase	−2.2	<0.0001
AV336704	Semaphorin 3B	−1.9	0.0001
M36411	Mpv17, glomerulosclerosis	−2.0	<0.0001
C78850	Envelope protein (env) gene	−2.0	<0.0001
AW049373	TCP-1 epsilon subunit	−1.8	<0.0001
M17192	Homeobox protein A7 (Hox-A7)	−1.7	0.0004
AB003305	Proteasome subunit, beta type 5	−1.8	<0.0001
U67188	Regulator of G-protein signaling 5	−1.7	0.0003
AB024922	Sarcoglycan, gamma	−1.6	<0.0001
AF084482	Wolfram syndrome gene	−1.6	0.0001
A1843119	Glutathione S-transferase like	−1.5	<0.0001
AV338260	Retinoblastoma 1	−1.5	0.0007
U07950	GDP dissociation inhibitor 1	−1.4	0.0124
Upregulated in BTBR-*ob/ob*			
Adipocytes specific genes			
U49915	Acrp30/adiponectin	1.6	<0.0001
M20497	aP2	1.6	<0.0001
AI326963	Fasting induced adipose factor	3.8	<0.0001
AA797604	Fasting induced adipose factor	1.6	0.0002
Y14004	Acyl-CoA thioesterase 1, cytosolic	1.6	<0.0001
M21285	Stearoyl-coenzyme A desaturase 1	2.1	<0.0001
U69543	Hormone sensitive lipase	1.5	0.0033
Metabolism			
AV255366	Ornithine decarboxylase	2.2	<0.0001
AI837005	Cdv3	1.4	0.0001
Z49204	Nicotinamide nucleotide transhydrogenase	1.7	<0.0001
X16670	Carbon catabolite repression 4 homolog	1.6	0.0005
X04120	Carbon catabolite repression 4 homolog	1.5	0.0018
K02236	Metaliothionein 2	1.5	<0.0001
Structure			
U68267	Myosin-binding protein H	1.5	0.0047
AF020185	Dynein, cytoplasmic, light chain 1	1.7	<0.0001
AV062363	Synuclein, gamma	1.6	0.0007
AA839903	Myosin light chain-2 isoform MLC-2a	1.6	<0.0001
J04953	Gelsolin	1.4	0.0055
AF051945	Cardiac morphogenesis	1.5	<0.0001
L08407	Procollagen, type XVII, alpha 1	1.8	0.0009
Others			
M64086	Serine protease inhibitor 2-2	2.3	<0.0001
AI848330	DNA segment ERATO Doi 689, expressed	1.9	<0.0001
U19118	Activating transcription factor 3	1.7	<0.0001
AF038939	Paternally expressed gene 3	1.6	<0.0001
AI854779	Nuclear ribonucleoprotein A/B	1.6	0.0005
M17551	Intracisternal A-particle gag protein	1.3	0.0050

highly expressed in leptin-deficient diabetic BTBR-*ob/ob* mice compared with leptin-deficient nondiabetic B6-*ob/ob* mice. The genes include cytokine subfamily B13 (AF030636), small inducible cytokine A7 (X70058) and A21a (AF035684), interferon-activated gene 202A (M31418), and interferon-inducible GTPase (AJ007971) (Table 1*A*).

Because a whole fat pad was used to isolate RNA for adipose tissue in this study, it is not clear whether the elevated signals of inflammatory genes are caused by an enrichment of macrophages in the fat pad of BTBR-*ob/ob* mice or are a result of elevated expression in the adipocytes. Taken together, the observation that acute-phase genes are turned on in leptin-deficient animals (4), and that the expression of macrophage markers is further

TABLE 4
Genes differentially expressed in pancreatic islets diabetic BTBR-*ob/ob* mice

Accession	Description	Fold	*P*
Downregulated in BTBR-*ob/ob*			
AF003525	Defensin beta 1	−4.2	<0.0001
AW050141	Adracalin	−3.0	<0.0001
X04573	Elastase 2	−2.8	<0.0001
AF009513	Plasma glutamate carboxypeptidase	−2.0	0.0012
M13660	Interferon alpha family, gene 9	−2.2	0.0001
X13333	CD14 antigen	−5.6	<0.0001
X05862	H2B histone gene	−2.2	<0.0001
AW121609	ATP-binding cassette, sub-family B12	−2.0	0.0010
M62374	γ-aminobutyric acid receptor	−1.8	0.0388
AF088983	Heat shock protein cognate 40	−1.8	0.0213
L34214	Regulated endocrine-specific protein 18	−1.8	0.0067
Upregulated in BTBR-*ob/ob*			
Metabolism			
AW124932	HMG-CoA synthase	1.8	0.0165
X95279	SPOT14	1.9	0.0013
U05809	Transketolase	2.4	0.0145
AA879764	NADH:ubiquinone oxidoreductase	2.1	<0.0001
AI846934	Lipin 1	2.5	<0.0001
AI790931	Fructose-1, 6-bisphosphatase 1	5.1	<0.0001
D42083	Fructose-1, 6-bisphosphatase 2	3.3	0.0005
L09104	Glucose phosphate isomerase 1	2.1	<0.0001
AF007267	Phosphomannomutase 1	4.6	<0.0001
AV318100	Glucosidase 1	2.3	<0.0001
U75215	Neutral amino acid transporter	2.3	<0.0001
U24428	Glulathione S-transferase, mu 5	1.8	0.0197
Secretory proteins			
X59520	Cholecystokinin	8.7	<0.0001
AE000665	Trypsin 2	3.5	<0.0001
AE000663	Trypsin-like serine protease	6.3	<0.0001
K02782	Complement component 3	2.4	<0.0001
X06342	Serine protease inhibitor, Kazal type 3	3.7	<0.0001
D63359	Pancreatitis-associated protein	2.9	<0.0001
Signal transduction			
AI845798	Phospholipase A2	2.5	<0.0001
AI642389	ER lumen protein retaining receptor 3	1.9	0.0032
AW048937	CDK inhibitor 1A (P21)	1.8	0.0172
AI196645	Rap7a	1.7	0.0064
Extracellular matrix			
AI527354	Fibronectin 1	3.4	<0.0001
AV374020	Keratin complex 1, acidic, gene 10	2.7	<0.0001
U03419	Procollagen, type 1, alpha 1	2.2	0.0243
U66166	Extracellular matrix protein 2	2.2	<0.0001
Others			
U48398	Aquaporin 4	1.8	0.0200
AI851345	Septin 7	2.3	0.0001
X52643	Histocompatibility 2A, alpha	2.7	0.0006
X61454	I3 protein	2.2	<0.0001
AJ243851	LIM homeobox protein 9	2.1	<0.0001
U19118	Activating transcription factor 3	2.0	0.0001
X96518	Homeo box, msh-like 3	2.0	0.0001
L26479	Translation elongation factor 1 alpha 2	1.9	0.0001
AJ242663	Cathepsin Z	1.8	0.0497
M89797	MMTV integration site 4	1.9	0.0024
AI854482	Mouse jerky gene (Jh8), epilepsy gene	1.7	0.0119

increased in diabetes, suggests a correlation between inflammation and the disease process. We propose that these abnormalities are related to increasing insulin resistance in adipose tissue. The link between individual cytokines and insulin resistance has previously been reported. Cytokines such as tumor necrosis factor-α, interleukin (IL)-1β, IL-6, and CD36 are major regulators of adipose

tissue metabolism (20,21). Adipose tissue expression of these genes is positively correlated with obesity-related insulin resistance (22). A recently identified insulin resistance marker, resistin (23), also known as *Fizz3*, is structurally related to a marker of inflammation, *Fizz1* (24).

The reduction of lipogenic gene expression in the BTBR-*ob/ob* mice cannot be simply explained by insulin defi-
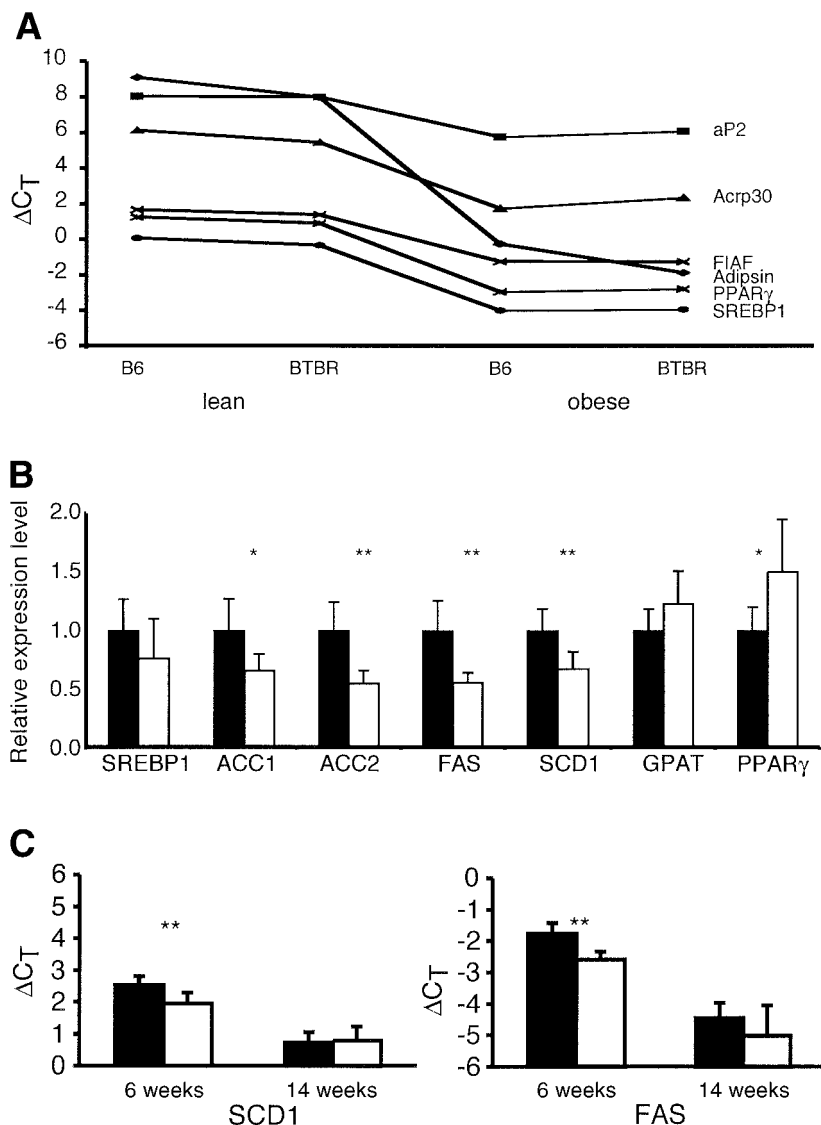
FIG. 3. *A*: Adipogenic gene expression in adipose tissue of 14-week-old lean and obese mice. Each data point is averaged from four mice. For the highly abundant adipocyte genes *aP2*, adipsin, and *ACRP30*, cDNA templates were diluted $2^8 = 256$-fold before placing into the RT-PCR to ensure the C_T values generated from these genes fall into a linear range. The *y*-axis is ΔC_T, which is comparable to the log-transformed, normalized mRNA abundance. *B*: Expression of lipogenic genes in the adipose tissue of 6-week-old B6-*ob/ob* ($n = 8$) and BTBR-*ob/ob* ($n = 6$) mice. The *y*-axis is the relative expression level normalized against the expression level in B6-*ob/ob*. ■, B6-*ob/ob*; □, BTBR-*ob/ob*. *$P < 0.05$, **$P < 0.01$. *C*: Time course expression of *SCD1* and *FAS* in adipose tissue. The *y*-axis is ΔC_T, which is comparable to the log-transformed, normalized mRNA abundance. ■, B6-*ob/ob*; □, BTBR-*ob/ob*. *$P < 0.05$, **$P < 0.01$.

ciency. At 6 weeks, BTBR-*ob/ob* mice had higher fasting insulin levels than B6-*ob/ob* mice. At 14 weeks, BTBR-*ob/ob* insulin levels dropped, whereas B6-*ob/ob* levels continued to rise. However, at both ages there was reduced expression of SREBP1 and its target genes in the livers of BTBR-*ob/ob* mice. The difference in gluconeogenic gene expression correlated with insulin levels. In prediabetic BTBR-*ob/ob* mice, where the insulin level was high, hepatic expression of *FBPase1* was lower than in the nondiabetic B6-*ob/ob* mice. When BTBR-*ob/ob* mice decompensated, the expression of *PEPCK* was elevated to a higher level than that of the B6-*ob/ob* mice. The increased gluconeogenesis in liver of BTBR-*ob/ob* mice is therefore adaptive to the reduced insulin level.

Intriguingly, hepatic steatosis is inversely correlated with diabetes susceptibility in obese mice. B6-*ob/ob* mice maintained euglycemia along with increasing hepatic steatosis, whereas BTBR-*ob/ob* mice had no fatty liver but were severely diabetic. We propose that increased lipogenesis in B6-*ob/ob* mice, although undesirable when it leads to hepatic steatosis, is protective against the development of diabetes. Supporting evidence for this concept has recently emerged in the literature. For example, the

PPAR-γ agonist GW1929, when administrated to Zucker diabetic fatty rats, increased the expression of several genes involved in lipogenesis (*FAS*, ATP-citrate lyase, *SCD1*, and acyl-CoA synthetase) in the liver (25). GW1929 produced fatty liver while ameliorating hyperglycemia. Similar observations have been reported for the antidiabetic thiazolidinediones in various mouse models of obesity and diabetes (26–28). In addition, Yahagi et al. (29) recently reported that the absence of *SREBP1* in B6-*ob/ob* mice ameliorates fatty liver but not obesity or insulin resistance, suggesting that fatty liver is not a cause of insulin resistance. Although hepatic steatosis was interpreted as a "side effect" of thiazolidinedione antidiabetic drugs (30), it may well comprise a part of their antidiabetic action.

Increased hepatic lipogenesis is also associated with reduced risk of diabetes in a lipoatrophic mouse model. The lipoatrophic A-ZIP/F-1 mouse was produced by adipose-selective expression of a dominant-negative protein (A-ZIP/F) that blocks the DNA binding of B-ZIP transcription factors of both the *C/EBP* and *Jun* families (31). Recently, Colombo et al. (32) compared the phenotype of the A-ZIP/F-1 (FVB) mutation on the FVB/N and B6 genetic
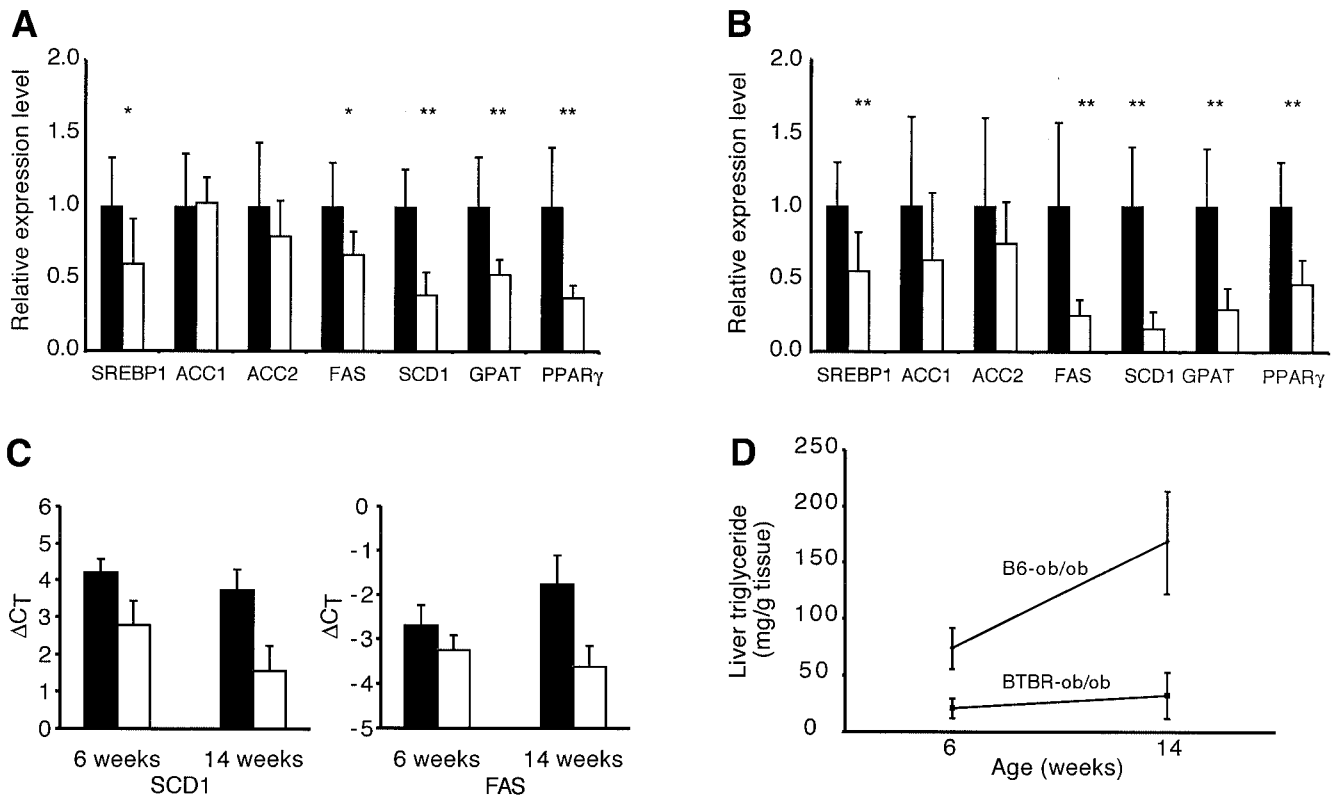
FIG. 4. *A*: Expression of lipogenic genes in the livers of 6-week-old female B6-*ob/ob* (*n* = 8) and BTBR-*ob/ob* (*n* = 6) mice. The *y*-axis is relative expression level normalized against the expression level in B6-*ob/ob* mice. ■, B6-*ob/ob*; □, BTBR-*ob/ob*. *$*P* < 0.05, **$*P* < 0.01. *B*: Expression of lipogenic genes in the livers of 14-week-old male B6-*ob/ob* (*n* = 10) and BTBR-*ob/ob* (*n* = 12) mice. The *y*-axis is the relative expression level normalized against the expression level in B6-*ob/ob* mice. ■, B6-*ob/ob*; □, BTBR-*ob/ob*. *$*P* < 0.05, **$*P* < 0.01. *C*: Time course expression of *SCD1* and *FAS* in liver. The *y*-axis is ΔC_T, which is comparable to the log-transformed, normalized mRNA abundance. ■, B6-*ob/ob*; □, BTBR-*ob/ob*. *$*P* < 0.05, **$*P* < 0.01. *D*: Liver TG content of B6-*ob/ob* and BTBR-*ob/ob* mice. The insulin levels for the mice studied in this experiment are as follows: 6-week-old female B6-*ob/ob* = 9.1 ± 7.1 ng/ml (*n* = 8); 6-week-old female BTBR-*ob/ob* = 24.7 ± 11.8 ng/ml (*n* = 6); 14-week-old male B6-*ob/ob* = 29.4 ± 22.1 ng/ml (*n* = 8); and 14-week-old male BTBR-*ob/ob* = 11.6 ± 8.9 ng/ml (*n* = 8).

backgrounds. FVB A-ZIP/F1 mice did not have fatty liver and they were severely diabetic. On the other hand, B6 A-ZIP mice showed increased levels of mRNA of lipogenic genes and a higher liver TG content, but no hyperglycemia. These observations are strikingly similar to what we have found in obese mouse models. Hepatic steatosis is therefore correlated with a lower risk of diabetes in both lipoatrophic and obese mouse models.

How might increased lipogenic capacity in the liver protect against the development of diabetes in both lipoatrophic and obese mice? A direct benefit of increased hepatic lipogenesis to the obese mice may involve alter-
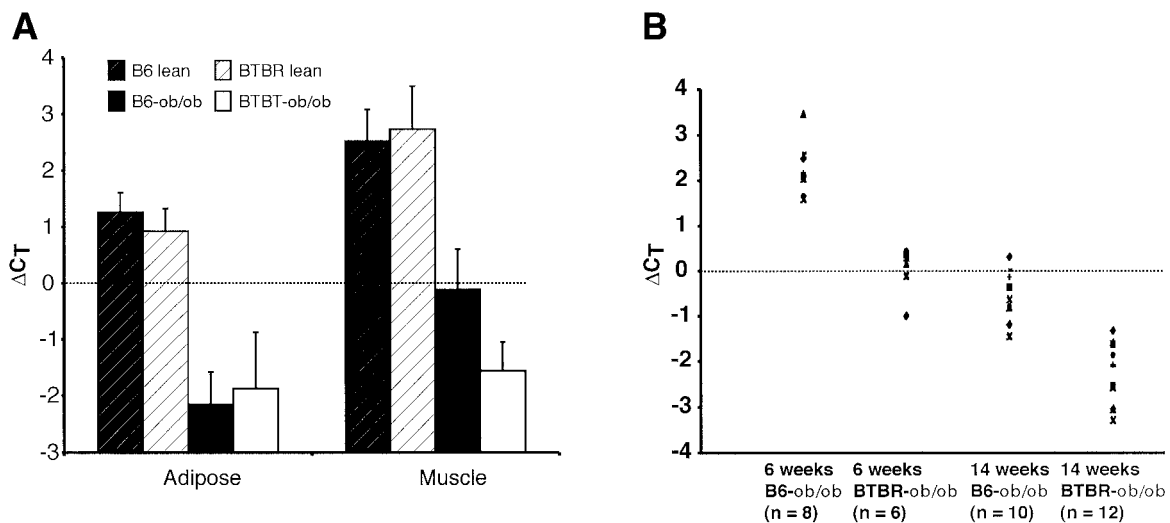

FIG. 5. Expression of ACO in adipose tissue and muscle of lean and obese B6 and BTBR mice (*A*) and in the liver of B6-*ob/ob* and BTBR-*ob/ob* mice (*B*) at 6 weeks and 14 weeks. Each dot in the graph represents a liver cDNA sample from an individual mouse. The *y*-axis is ΔC_T. The dotted line represents the expression level of the β-actin gene, which serves as a normalization control.
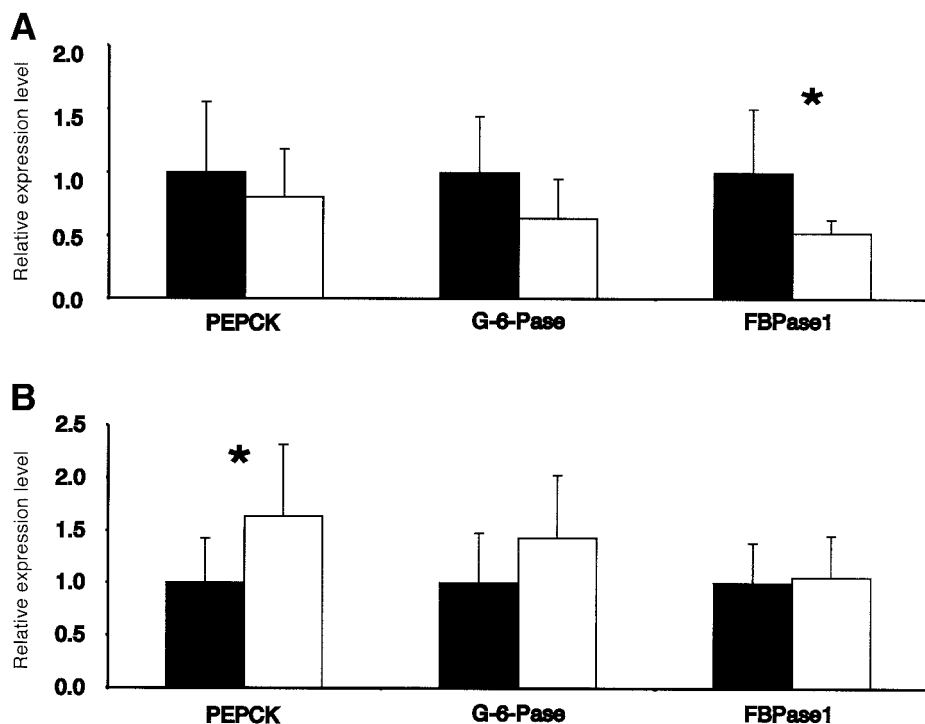
FIG. 6. Expression of gluconeogenic genes in BTBR-*ob/ob* liver at 6 weeks (*A*) and 14 weeks (*B*). The *y*-axis is the relative expression level normalized against the expression level in B6-*ob/ob*. ■, B6-*ob/ob*; □, BTBR-*ob/ob*. *$P < 0.05$.

ations in fuel partitioning. Both B6-*ob/ob* and BTBR-*ob/ob* mice are leptin deficient. The animals have high food intake and low energy consumption. Thus, there is accumulation of excess nutrient, which has to be stored in lipid or might contribute to increased glucose production. Elevating the lipogenic pathway in the liver may help to deter metabolic partitioning into the gluconeogenic pathway, thus reducing the rate of glucose production in the liver. Recently, Becard et al. (33) reported the phenotype of recombinant adenovirus-mediated hepatic overexpression of *SREBP-1c* in streptozotocin-induced diabetic mice. The study showed that increased hepatic lipogenesis leads to a marked reduction in hyperglycemia in diabetic mice. The treatment induced lipogenic enzyme gene expression and increased liver TG content. Meanwhile, it repressed the expression of PEPCK, so that glucose homeostasis was greatly improved (33). More recently, Cao et al. (34) reported that diabetic rodents treated with a liver X receptor agonist developed increased liver TGs and normalized their plasma glucose levels.

We do not know whether the mass of lipid produced de novo is sufficient to significantly alter the flux through the gluconeogenic pathway. It is also conceivable that the products of the lipogenesis pathway might be partitioned to key regulatory sites of whole-body metabolism that could alter diabetes susceptibility. Reduced lipogenesis in adipose tissue is a common feature in these obese mice, and it may play an important physiological role. In obese mice and humans, adipose tissue, although large in size, has reduced lipogenic capacity, in part a consequence of reduced expression of *SREBP-1c* (4–9). In this study, we showed that the adipocyte lipogenic genes are dysregulated with prolonged obesity (Fig. 3*C*). We also show that obese mice have reduced expression of fatty acid oxidation genes (Fig. 5), suggesting a reduced capacity for lipid catabolism. The increased hepatic lipogenesis in lipoatrophy and obesity (8,10) constitutes a major shift of lipo-

genic burden from the adipose tissue to the liver (11). Some studies have shown a correlation between TG overaccumulation in nonadipose tissues (e.g., skeletal muscle) and insulin resistance (35–38). TG accumulation in pancreatic islets might cause β-cell lipoapoptosis and diabetes (39,40). TG accumulation in the liver may therefore prevent lipid deposition elsewhere and lipotoxic damage to the pancreatic islets.

Recently, Busch et al. (41) reported the expression profile of the β-cell line MIN6 treated with palmitate and oleate. Similar to what we have seen in our in vivo study, they also observed that genes not normally in pancreatic islets, such as *FBPase1* and *FBPase2*, are induced under chronic lipid exposure. In both studies, a decrease in *GLUT2* expression was observed. These results raise the possibility that the BTBR-*ob/ob* islets might undergo lipotoxic damage. Compared with nondiabetic B6-*ob/ob* mice, BTBR-*ob/ob* females show a lower liver TG content but a significantly higher plasma TG level. The difference arises before the onset of hyperglycemia and progresses with the onset of diabetes.

REFERENCES

1. Coleman DL, Hummel KP: The influence of genetic background on the expression of the obese (Ob) gene in the mouse. *Diabetologia* 9:287–293, 1973
2. Stoehr JP, Nadler ST, Schueler KL, Rabaglia ME, Yandell BS, Metz SA, Attie AD: Genetic obesity unmasks nonlinear interactions between murine type 2 diabetes susceptibility loci. *Diabetes* 49:1946–1954, 2000
3. Ranheim T, Dumke C, Schueler KL, Cartee GD, Attie AD: Interaction between BTBR and C57BL/6J genomes produces an insulin resistance syndrome in (BTBR x C57BL/6J) F1 mice. *Arterioscler Thromb Vasc Biol* 17:3286–3293, 1997

4. Soukas A, Cohen P, Socci ND, Friedman JM: Leptin-specific patterns of gene expression in white adipose tissue. *Genes Dev* 14:963–980, 2000

5. Nadler ST, Stoehr JP, Schueler KL, Tanimoto G, Yandell BS, Attie AD: The expression of adipogenic genes is decreased in obesity and diabetes mellitus. *Proc Natl Acad Sci U S A* 97:11371–11376, 2000

6. Ducluzeau PH, Perretti N, Laville M, Andreelli F, Vega N, Riou JP, Vidal H: Regulation by insulin of gene expression in human skeletal muscle and adipose tissue: evidence for specific defects in type 2 diabetes. *Diabetes* 50:1134–1142, 2001

7. Kolehmainen M, Vidal H, Alhava E, Uusitupa MI: Sterol regulatory element binding protein 1c (SREBP-1c) expression in human obesity. *Obes Res* 9:706–712, 2001

8. Diraison F, Dusserre E, Vidal H, Sothier M, Beylot M: Increased hepatic lipogenesis but decreased expression of lipogenic gene in adipose tissue in human obesity. *Am J Physiol Endocrinol Metab* 282:E46–E51, 2002

9. Sewter C, Berger D, Considine RV, Medina G, Rochford J, Ciaraldi T, Henry R, Dohm L, Flier JS, O'Rahilly S, Vidal-Puig AJ: Human obesity and type 2 diabetes are associated with alterations in SREBP1 isoform expression that are reproduced ex vivo by tumor necrosis factor-alpha. *Diabetes* 51:1035–1041, 2002

10. Shimomura I, Bashmakov Y, Horton JD: Increased levels of nuclear SREBP-1c associated with fatty livers in two mouse models of diabetes mellitus. *J Biol Chem* 274:30028–30032, 1999

11. Nadler ST, Attie AD: Please pass the chips: genomic insights into obesity and diabetes. *J Nutr* 131:2078–2081, 2001

12. Li C, Wong WH: Model-based analysis of oligonucleotide arrays: expression index computation and outlier detection. *Proc Natl Acad Sci U S A* 98:31–36, 2001

13. Lin Y, Nadler ST, Lan H, Attie AD, Yandell BS: Adaptive gene picking with microarray data: detecting important low abundance signals. In *The Analysis of Gene Expression Data: Methods and Software*. Parmigiani ES, Garrett RA, Irizarry SL, Eds. New York, Springer-Verlag, 2002

14. Briaud I, Harmon JS, Kelpe CL, Segu VB, Poitout V: Lipotoxicity of the pancreatic beta-cell is associated with glucose-dependent esterification of fatty acids into neutral lipids. *Diabetes* 50:315–321, 2001

15. Newton MA, Kendziorski CM, Richmond CS, Blattner FR, Tsui KW: On differential variability of expression ratios: improving statistical inference about gene expression changes from microarray data. *J Comput Biol* 8:37–52, 2001

16. Cook KS, Min HY, Johnson D, Chaplinsky RJ, Flier JS, Hunt CR, Spiegelman BM: Adipsin: a circulating serine protease homolog secreted by adipose tissue and sciatic nerve. *Science* 237:402–405, 1987

17. Peterfy M, Phan J, Xu P, Reue K: Lipodystrophy in the fld mouse results from mutation of a new gene encoding a nuclear protein, lipin. *Nat Genet* 27:121–124, 2001

18. Borriello F, Krauter KS: Multiple murine alpha 1-protease inhibitor genes show unusual evolutionary divergence. *Proc Natl Acad Sci U S A* 88:9417–9421, 1991

19. Tardiff J, Krauter KS: Divergent expression of alpha1-protease inhibitor genes in mouse and human. *Nucleic Acids Res* 26:3794–3799, 1998

20. Fruhbeck G, Gomez-Ambrosi J, Muruzabal FJ, Burrell MA: The adipocyte: a model for integration of endocrine and metabolic signaling in energy metabolism regulation. *Am J Physiol Endocrinol Metab* 280:E827–E847, 2001

21. Coppack SW: Pro-inflammatory cytokines and adipose tissue. *Proc Nutr Soc* 60:349–356, 2001

22. Kern PA, Ranganathan S, Li C, Wood L, Ranganathan G: Adipose tissue tumor necrosis factor and interleukin-6 expression in human obesity and insulin resistance. *Am J Physiol Endocrinol Metab* 280:E745–E751, 2001

23. Steppan CM, Bailey ST, Bhat S, Brown EJ, Banerjee RR, Wright CM, Patel HR, Ahima RS, Lazar MA: The hormone resistin links obesity to diabetes. *Nature* 409:307–312, 2001

24. Holcomb IN, Kabakoff RC, Chan B, Baker TW, Gurney A, Henzel W, Nelson C, Lowman HB, Wright BD, Skelton NJ, Frantz GD, Tumas DB, Peale FV Jr, Shelton DL, Hebert CC: FIZZ1, a novel cysteine-rich secreted protein associated with pulmonary inflammation, defines a new gene family. *Embo J* 19:4046–4055, 2000

25. Way JM, Harrington WW, Brown KK, Gottschalk WK, Sundseth SS, Mansfield TA, Ramachandran RK, Willson TM, Kliewer SA: Comprehensive messenger ribonucleic acid profiling reveals that peroxisome proliferator-activated receptor gamma activation has coordinate effects on gene expression in multiple insulin-sensitive tissues. *Endocrinology* 142:1269–1277, 2001

26. Suzuki A, Yasuno T, Kojo H, Hirosumi J, Mutoh S, Notsu Y: Alteration in expression profiles of a series of diabetes-related genes in db/db mice following treatment with thiazolidinediones. *Jpn J Pharmacol* 84:113–123, 2000

27. Bedoucha M, Atzpodien E, Boelsterli UA: Diabetic KKAy mice exhibit increased hepatic PPARgamma1 gene expression and develop hepatic steatosis upon chronic treatment with antidiabetic thiazolidinediones. *J Hepatol* 35:17–23, 2001

28. Chao L, Marcus-Samuels B, Mason MM, Moitra J, Vinson C, Arioglu E, Gavrilova O, Reitman ML: Adipose tissue is required for the antidiabetic, but not for the hypolipidemic, effect of thiazolidinediones. *J Clin Invest* 106:1221–1228, 2000

29. Yahagi N, Shimano H, Hasty AH, Matsuzaka T, Ide T, Yoshikawa T, Amemiya-Kudo M, Tomita S, Okazaki H, Tamura Y, Iizuka Y, Ohashi K, Osuga J, Harada K, Gotoda T, Nagai R, Ishibashi S, Yamada N: Absence of sterol regulatory element-binding protein-1 (SREBP-1) ameliorates fatty livers but not obesity or insulin resistance in Lep(ob)/Lep(ob) mice. *J Biol Chem* 277:19353–19357, 2002

30. Boelsterli UA, Bedoucha M: Toxicological consequences of altered peroxisome proliferator-activated receptor gamma (PPARgamma) expression in the liver: insights from models of obesity and type 2 diabetes. *Biochem Pharmacol* 63:1–10, 2002

31. Moitra J, Mason MM, Olive M, Krylov D, Gavrilova O, Marcus-Samuels B, Feigenbaum L, Lee E, Aoyama T, Eckhaus M, Reitman ML, Vinson C: Life without white fat: a transgenic mouse. *Genes Dev* 12:3168–3181, 1998

32. Colombo C, Haluzik M, Cutson JJ, Dietz KR, Marcus-Samuels B, Vinson C, Gavrilova O, Reitman ML: Opposite effects of background genotype on muscle and liver insulin sensitivity of lipoatrophic mice: role of triglyceride clearance. *J Biol Chem*. In press

33. Becard D, Hainault I, Azzout-Marniche D, Bertry-Coussot L, Ferre P, Foufelle F: Adenovirus-mediated overexpression of sterol regulatory element binding protein-1c mimics insulin effects on hepatic gene expression and glucose homeostasis in diabetic mice. *Diabetes* 50:2425–2430, 2001

34. Cao G, Liang Y, Broderick CL, Oldham BA, Beyer TP, Schmidt RJ, Zhang Y, Stayrook KR, Suen C, Otto KA, Miller AR, Dai J, Foxworthy P, Gao H, Ryan TP, Jiang XC, Burris TP, Eacho PI, Etgen GJ: Antidiabetic action of a liver X receptor agonist mediated by inhibition of hepatic gluconeogenesis. *J Biol Chem* 278:1131–1136, 2003

35. Kelley DE, Goodpaster BH: Skeletal muscle triglyceride: an aspect of regional adiposity and insulin resistance (Review). *Diabetes Care* 24:933–941, 2001

36. McGarry JD: Banting Lecture 2001: Dysregulation of fatty acid metabolism in the etiology of type 2 diabetes. *Diabetes* 51:7–18, 2002

37. Yu C, Chen Y, Zong H, Wang Y, Bergeron R, Kim JK, Cline GW, Cushman SW, Cooney GJ, Atcheson B, White MF, Kraegen EW, Shulman GI: Mechanism by which fatty acids inhibit insulin activation of insulin receptor substrate-1 (IRS-1)-associated phosphatidylinositol 3-kinase activity in muscle. *J Biol Chem* 277:50230–50236, 2002

38. Kim JK, Fillmore JJ, Chen Y, Yu C, Moore IK, Pypaert M, Lutz EP, Kako Y, Velez-Carrasco W, Goldberg IJ, Breslow JL, Shulman GI: Tissue-specific overexpression of lipoprotein lipase causes tissue-specific insulin resistance. *Proc Natl Acad Sci U S A* 98:7522–7527, 2001

39. Unger RH: Lipotoxic diseases. *Ann Rev Med* 53:319–336, 2002

40. Unger RH, Zhou YT, Orci L: Regulation of fatty acid homeostasis in cells: novel role of leptin. *Proc Natl Acad Sci U S A* 96:2327–2332, 1999

41. Busch AK, Cordery D, Denyer GS, Biden TJ: Expression profiling of palmitate- and oleate-regulated genes provides novel insights into the effects of chronic lipid exposure on pancreatic β-cell function. *Diabetes* 51:977–987, 2002